Bridge Maintenance, Safety, Management, Digitalization and Sustainability – Jensen, Frangopol & Schmidt (eds)

Load testing of the first stress ribbon bridge in Slovenia

Đ. Đukić, D. Hekič, M. Kosič, R. Vezočnik & A. Anžlin
Slovenian National Building and Civil Engineering Institute, Ljubljana, Slovenia

A. Štrukelj
Faculty of Civil Engineering, Transportation Engineering and Architecture, University of Maribor, Maribor, Slovenia

M. Pipenbaher & T. Weingerl
Ponting inženirski biro, Maribor, Slovenia

ABSTRACT: Paper presents selected results of the diagnostic load testing of a newly-built footbridge in Novo Mesto, Slovenia. The bridge is significant as the first bridge in Slovenia being built with the stress ribbon technology. The diagnostic load testing took place in March 2023 and comprised of three-stage static load testing, dynamic testing with a light truck driving over artificial obstacles, and measurement of ambient vibrations. The consistency between the actual response of the bridge and the response of the finite element (FE) model, used in the design, was evaluated by comparing vertical displacements from the static load testing, natural frequencies and mode shapes. The comparison of the results indicates a satisfactory agreement between the measurements and the response of the FE model, confirming the appropriateness of the employed FE model.

1 INTRODUCTION

A newly built pedestrian bridge in the village of Irča Vas, near Novo Mesto, is the first bridge in Slovenia built using stress-ribbon technology. The bridge is a slender catenary-shaped structure with concrete precast segments placed over prestressed steel ribbons that function as scaffolding during bridge construction (Strasky & Pirner, 1986). Forces from the stress ribbons are transferred through well foundations and geotechnical anchors on both sides of the bridge to load-bearing soil.

In March 2023, a diagnostic load test was conducted using 18 3.9-tonne trucks, representing approximately 60% of the design load. Proof load tests in the USA should be performed using guidelines set by the Manual for Bridge Evaluation (2018). Similar approach was utilised in the case of Irča Vas bridge. To validate the designer's calculations, an extensive measurement campaign was undertaken. It is comprised of sensors installed for long-term monitoring and sensors installed for diagnostic load tests, designated as short-term measurements. The following measurements were performed: measurement of rotations using inclinometers and 3-axial MEMS accelerometers, acceleration measurements using single and 3-axial MEMS accelerometers, and deflection measurements using a total station and 3D laser scanner. Additionally, force in the geotechnical anchors was measured. This article outlines the most important results of the diagnostic load testing with a focus on short-term sensor data and compares with the calculated response from the bridge designer's finite element (FE) model.

2 BRIDGE DESCRIPTION

A new pedestrian bridge crosses the Krka river with a span of 131 m, as shown in Figure 1. The maximum longitudinal slope of the bridge is 6%, as the structure has an inbuilt radius, where its lowest point is around 8 m above the river surface.

DOI: 10.1201/9781003483755-45

Figure 1. Bridge on the day of the diagnostic load test.

The bridge deck is supported with abutments, which rest upon the well foundations. The tensile forces from prestressing tendons are carried over by geotechnical anchors and transferred in load-bearing soil (Figure 2).

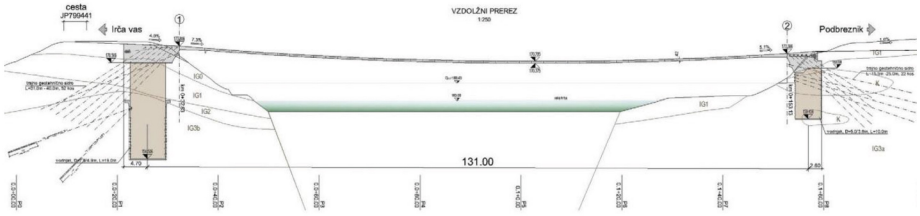

Figure 2. Longitudinal section of the bridge.

The cross-section of the bridge is shown in Figure 3. Precast concrete elements are 4.0 m wide and 2.4 m long. Element thickness varies in a transverse direction from 0.42 m at the edges to 0.18 m in the middle. The usable width of the bridge is 3.5 m. Precast elements are built offsite using C45/55 concrete. More in-depth information about the bridge geometry and building process is available in Weingerl et al. (2023).

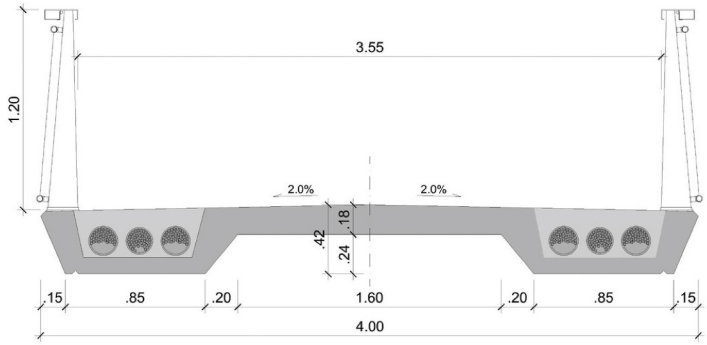

Figure 3. Cross-section of the bridge.

3 MEASUREMENTS

The bridge's diagnostic load test comprised static (trucks stationary on the bridge) and dynamic (trucks passing an artificial bump on the bridge) testing. In addition, vibrations

under ambient excitation before and after the testing campaign were captured. 6 phases were performed overall:

- Phase 0: Resting phase before loading (zero state).
- Phase 1: 9 trucks at the 2/2 of the bridge (half-load).
- Phase 2: 18 trucks across the entire bridge (full load of 70.4 tonnes overall, Figure 4).
- Phase 3: 9 trucks at the 1/2 of the bridge (half-load).
- Phase 4: Resting phase after loading (release state).
- Phase 5: Dynamic test – trucks passes artificial bump on the bridge.

Figure 4. In the static load test (Phase 2), all 18 trucks with an overall 70.4 tonnes were present on the bridge.

Axle loads and distance of statically-weighted 18 trucks are presented in Table 1.

Table 1. Axle load data for each truck used during the load test.

Truck number	Axle distance[m]	1st axle load[kg]	2nd axle load[kg]	SUM[kg]
1	4.35	1700	2200	3900
2	3.65	1600	2400	4000
3	3.65	1400	2800	4200
4	3.65	1500	2300	3800
5	3.00	1700	2200	3900
6	3.60	1600	2300	3900
7	4.35	1700	2300	4000
8	3.65	1300	2900	4200
9	3.65	1300	2900	4200
10	3.65	1400	2700	4100
11	3.65	1300	2900	4200
12	3.65	1500	1900	3400
13	3.65	1300	2700	4000
14	4.35	1700	1800	3500
15	3.65	1300	2700	4000
16	4.35	1700	1700	3400
17	3.65	1500	2300	3800
18	3.65	1500	2600	4100

During phase 0, zero state was measured with both total stations, 3D laser scanner, MEMS accelerometers (for inclinations) and inclinometers. Moreover, ambient vibrations were measured with MEMS accelerometers for a duration of approximately 20 minutes.

Phase 1 was conducted by placing the first 9 trucks on the 2nd half of the bridge, between the mid-span and end (left, according to Figure 4) abutment. Phase 2 was conducted without load relief by adding 9 additional trucks to the 1st half of the bridge, between the first abutments and the mid-span. Phase 3 of the static load test was performed by removing the 9 trucks from bridge such that trucks were only present in the 1st half of the bridge, between the right(according to the the Figure 4) abutment and the mid-span. In phase 4, the bridge was fully relieved. For Phase 1 – Phase 4 the vertical displacements of the deck and horizontal displacements of the abutments were measured with both total stations. Additionally, the inclinations of the deck were measured with MEMS accelerometers and the inclinations of the abutments with inclinometers. 3D laser scans were performed only for Phase 2 and Phase 4. Ambient vibrations using MEMS accelerometers were measured only in phase 4.

The aim of the dynamic test was to excite the structure such that modal parameters could also be determined with uniaxial accelerometers (presented in Chapter 4), which are permanently installed on the bridge, and not only with the MEMS accelerometers. During this test, a truck was driving over the four equally-distant wooden obstacles near the mid-span. In the first measurement, the truck crossed the bridge from right to left (according to Figure 4) abutment with 20 km/h. Afterwards, a truck drove in the reverse direction across the same obstacles at 10 km/h. In the last phase, the truck drove over the bridge in both directions at 10 km/h.

4 INSTRUMENTATION

The considered bridge has a built-in permanent monitoring system which is capable of continuous measurement of bridge accelerations and rotations of the abutments, as shown in Figure 5.

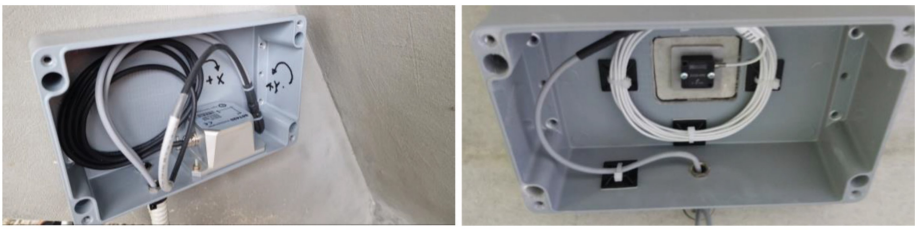

Figure 5. Sensors used for the permanent monitoring: biaxial inclinometer (left) and uniaxial accelerometer (right).

The permanent monitoring system is designed such that it allows for remote access to the measured data. Each abutment is equipped with one biaxial inclinometer (type Vigor Technology SST420), which allows for the measurement of support rotation (INCL_01 and INCL_02 in Figure 6). Uniaxial accelerometers used in permanent monitoring (type Silicon Designs 2220-002) are placed on the bottom side of the precast concrete elements of the bridge deck. They were placed before the precast elements in the construction phase due to the difficulty of access afterward. Three pairs of two accelerometers were placed at the narrower part of the bridge deck (ACC_01 – ACC_06 in Figure 6). Using those accelerometers, three cross-sections were instrumented (First quarter, middle quarter, and third quarter of the span). Due to vandalism which occurred after the construction and before the load test of the bridge, connection to accelerometer ACC_06 and inclinometer INCL_01 was lost, and it was impossible to re-establish after the end of the construction.

During the load test of the bridge, all working sensors that are part of the permanent monitoring system were used. Additionally, the bridge was temporarily equipped with 12 triaxial MEMS accelerometers (type DEWESoft IOLITEi 3xMEMS-ACC), designated with green dots in Figure 6). These accelerometers were placed in pairs every 20 m of the bridge and were used to identify modal parameters in Phase 0 and Phase 4.

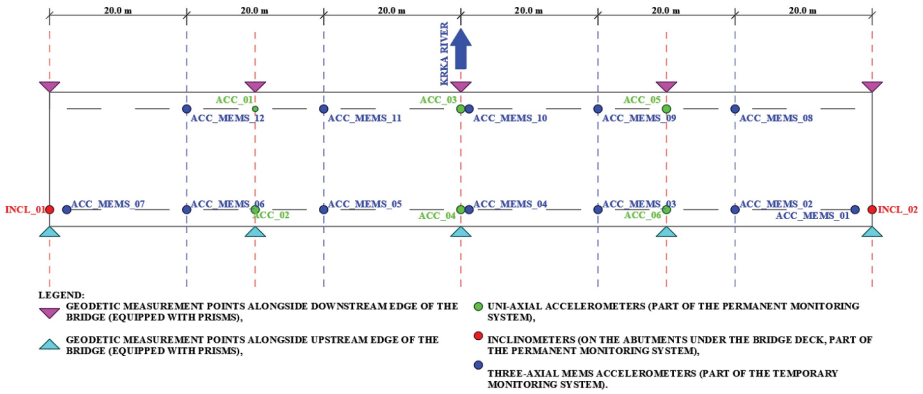

Figure 6. Sensor disposition (permanent and temporary monitoring systems).

During the static load test, vertical displacement along the upstream and downstream edge of the bridge was measured using two total stations and a laser scanner (Figure 7). Vertical displacement measurement points were placed along the upstream and downstream edges of the bridge deck at quarter, middle and three-quarters of the bridge span. Rotation of the abutments, horizontal displacements and rotations at the abutments were measured for all phases of the static load test.

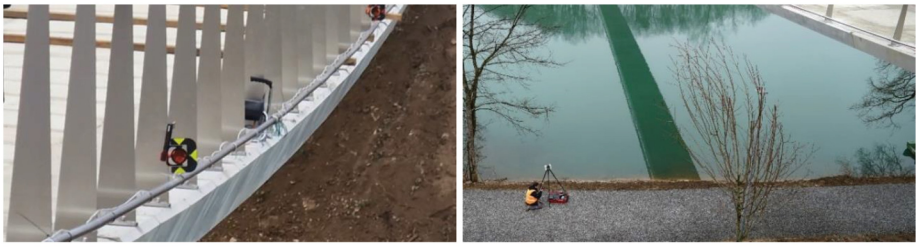

Figure 7. Geodetic measurement points along the downstream edge of the bridge deck (left) and position of the laser scanner (right).

Laser scanning was carried out with a Leica RTC360 laser scanner situated at the upstream river bank. From this location, the instrument's range managed to include about 80 m of the bridge, reaching well beyond the structure's lowest point in the middle of the bridge (60 m). Due to such limited scanning geometry, the highest scanning resolution was selected (3 mm at a distance of 10 m), resulting in roughly 3000 points per square meter at the location of the lowest bridge point. The 3D point accuracy of this scanner at a distance of 60 m is about 5 mm. One should note, however, that since only relative displacements in the vertical direction were of primary interest, this value is not completely representative.

5 MEASUREMENT RESULTS AND COMPARISON

Each of the measured parameters was calculated by the designer during the design phase of the project. A detailed FE model was created in SOFISTIK software. Before the load test phase, the designers also calculated the vertical displacement of the deck, abutment rotations and horizontal abutment displacement for each of the three phases of the static load test. Alongside the displacements, the designer calculated modal characteristics, namely the natural frequencies and mode shapes, beforehand. Below are the most important results, i.e., a comparison of the mid-span

deflection and modal characteristics measurements. More in-depth analysis exceeds the scope of this paper.

A comparison between the calculated and measured bridge deck vertical displacements for all three static load cases is shown in Table 2. The values shown represent the average displacement of the downstream and upstream edges of the bridge deck.

The scanning was carried out in three consecutive time moments, i.e. before the loading (T1 designating Phase 0), at the time of the maximum load (T2 designating Phase 2), and after unloading (T3 designating Phase 3). Two distinct point profiles (P1 and P2) were selected from these three point clouds on each side of the bridge deck, forming the basis for further bridge displacement analysis. The P1 point profile consists of points near the upstream edge of the deck, and the P2 point profile consists of points near the downstream edge of the deck. Both profiles are 5 centimetres wide. The shape of each profile in the vertical domain was modelled using polynomials since they best fitted the profile points. Figure 8 shows the deformation line of the bridge deck's downstream edge for all three static load test phases.

Table 2. A comparison between the average measured and calculated values of mid-span vertical displacement of the bridge deck.

Phase	Total station [mm]	Laser scanner* [mm]	FE model [mm]
1	65.0	/	69.5
2	129.0	127.3	145.5
3	70.1	/	64.5
4	9.9	7.6	/

* average values of profiles P1 and P2

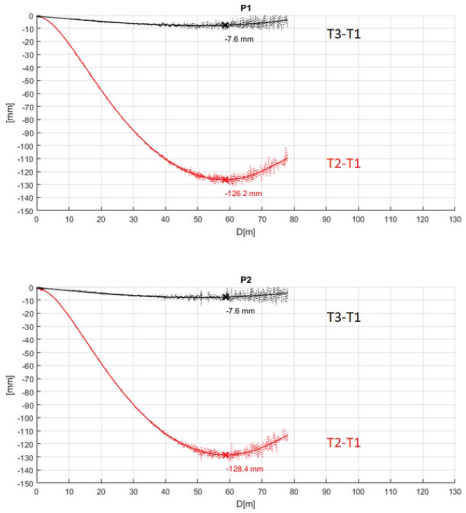

Figure 8. Measured deformation line of the downstream edge of the bridge deck for all three phases of static load test.

As shown in Table 2, the values of measured and calculated displacements match well for all three phases of the static load test. Measured displacements were smaller than calculated. Values measured by a laser scanner and total station differ by 2 mm. Figure 9 shows the point cloud measured with the laser scanner.

Table 3 shows the measured and calculated natural frequencies which correspond to the vertical mode shapes of the structure. Table 4 shows the measured and calculated mode

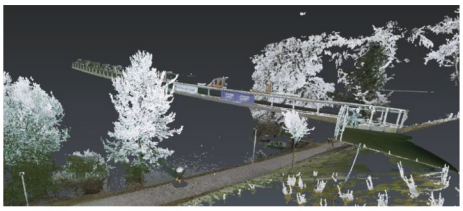

Figure 9. Point cloud measured with a laser scanner.

Table 3. First three measured and calculated natural frequencies [Hz].

Vertical mode shape	Measured – FDD	FE model
1	0.68	0.70
2	0.98	1.09
3	1.51	1.66

Table 4. Comparison between measured and FE model mode shapes.

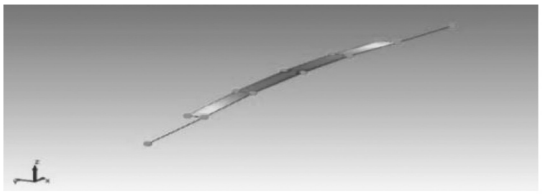

1st measured mode shape: f_1 = 0.68 Hz

1st FE model mode shape: f_2 = 0.70 Hz

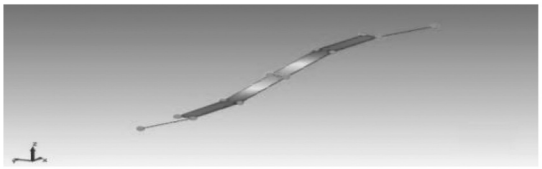

2nd measured mode shape: f_2 = 0.98 Hz

2nd FE model mode shape: f_3 = 1.09 Hz

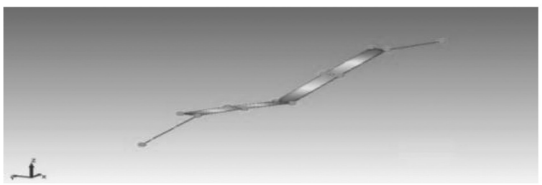

3rd measured mode shape: f_3 = 1.51 Hz

3rd FE model mode shape: f_3 = 1.66 Hz

shapes. Measured modal parameters were extracted with the Frequency Domain Decomposition (FDD) method (Brincker et al. 2000) using the ARTeMIS Modal (Structural Vibration Solutions 2023) software package for modal identification of structures.

As shown in Table 4, modal parameter identification methods give satisfactory estimates of natural frequencies. The best matching between measurements and the numerical model was recorded for the first mode shape. For the second and third mode shapes, natural frequencies were overestimated. Natural frequencies calculated using numerical models are for the first three mode shapes higher than those measured, which indicate the higher stiffness of the model. At most, measured and calculated natural frequencies differ by 11.2 % for the second mode shape.

6 CONCLUSIONS

The paper presents selected results of load testing of the newly built stress ribbon pedestrian bridge near Novo Mesto, Slovenia. The bridge is significant as the first bridge in Slovenia to be built using stress ribbon technology. Diagnostic load testing of the bridge consisted of three-phase static load testing, dynamic load testing performed with truck driving over artificial obstacles and ambient vibration measurements. Static response of the structure was recorded using two electronic total stations and a laser scanner. The dynamic response of the structure was measured using the permanent monitoring system, which includes uniaxial accelerometers and biaxial inclinometers, and a temporary monitoring system, which consists of 12 triaxial MEMS accelerometers. Furthermore, MEMS accelerometers were used to measure the response under ambient excitation before and after the load test.

Only the selected results are shown in this paper, mainly from the short-term measurements i.e. vertical displacement at the mid-span of the bridge and three vertical mode shapes and their corresponding natural frequencies. The matching between measured and calculated values of vertical displacement was satisfactory in all three phases of static load testing. Measured displacements were smaller than calculated ones. However, the order of magnitude was comparable. Additionally, satisfactory matching was also achieved between measured and calculated vertical mode shapes and their corresponding natural frequencies.

The findings of the load test confirm correct modelling and assumptions during the design of the bridge. For a better understanding of the complex static and dynamic response of the bridge, additional data analysis and calculations are required.

REFERENCES

American Association of State Highway Transportation Officials. 2018. The Manual for Bridge Evaluation, Standard, 3rd ed. AASHTO, Washington, D.C.

Brincker, R., Zhang, L. & Andersen, P. 2000. Modal identification from ambient responses using frequency domain decomposition. Proceeding of the International Modal Analysis Conference – IMAC, 7-10 February 2000, San Antonio, Texas, USA.

Strasky J. & Pirner, M. 1986. DS-L Stress-ribbon footbridges, Dobravni stavby, Olomouc, Czechoslovakia.

Structural Vibration Solutions. 2023. ARTeMIS Modal Pro [online]. Available from: https://www.svibs.com/artemis-modal-pro/ [Accessed 26 Dec 2023].

Weingerl, T., Pipenbaher, M., Gotovčević, T. & Filipič, A. 2023. Prvi most, grajen po tehnologiji natezнega traku v Sloveniji (in Slovene). Gradbeni vestnik letnik 72: 206–216.